Electronic Supplementary Material (ESI) for Journal of Materials Chemistry C.

Supporting Information

Gate-controlled multi-bit nonvolatile ferroelectric organic transistor memory on paper substrates

Meili Xu, Xindong Zhang, Shizhang Li, Ting Xu, Wenfa Xie and Wei Wang*

College of Electronic Science and Engineering, Jilin University, 2699 Qianjin Street, Changchun 130012, China

* E-mail: wwei99@jlu.edu.cn

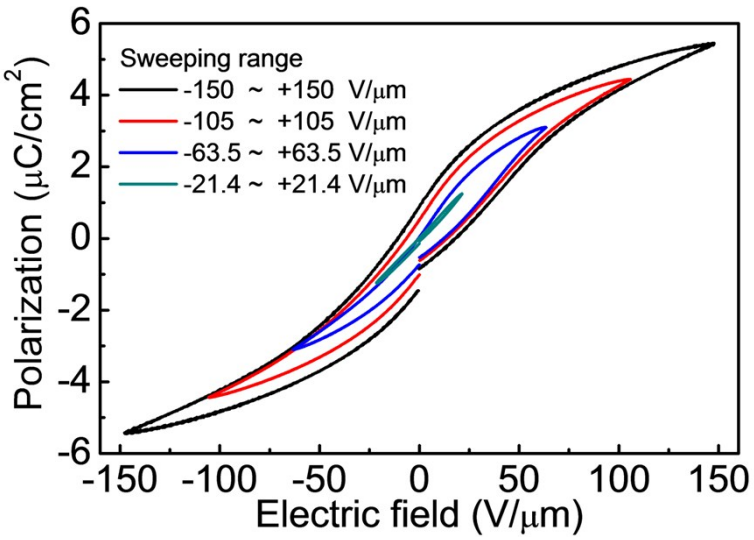

Figure S1. Polarization-electric field hysteresis properties of Al/P(VDF-TrFE-CTFE)/Au ferroelectric capacitors at different sweeping voltage ranges.

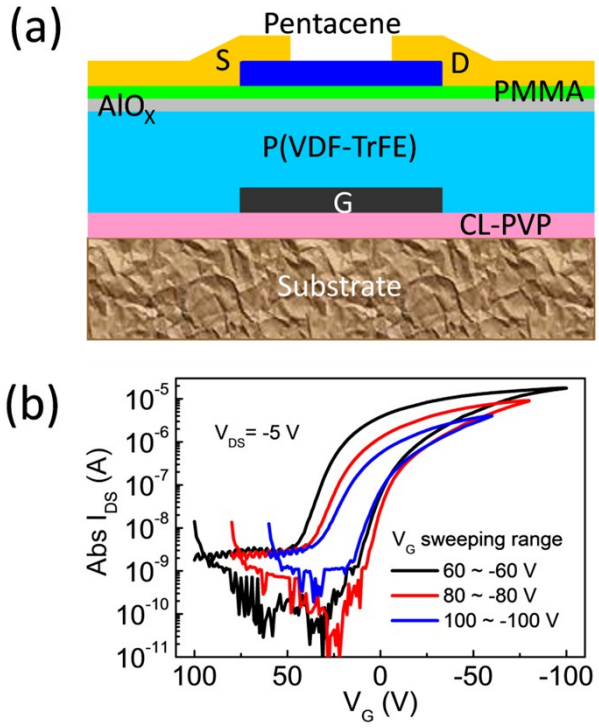

Figure S2. (a) Schematic diagram and (b) $I_{DS} - V_G$ transfer characteristics of the OFET with conventional P(VDF-TrFE) as the ferroelectric gate dielectric.

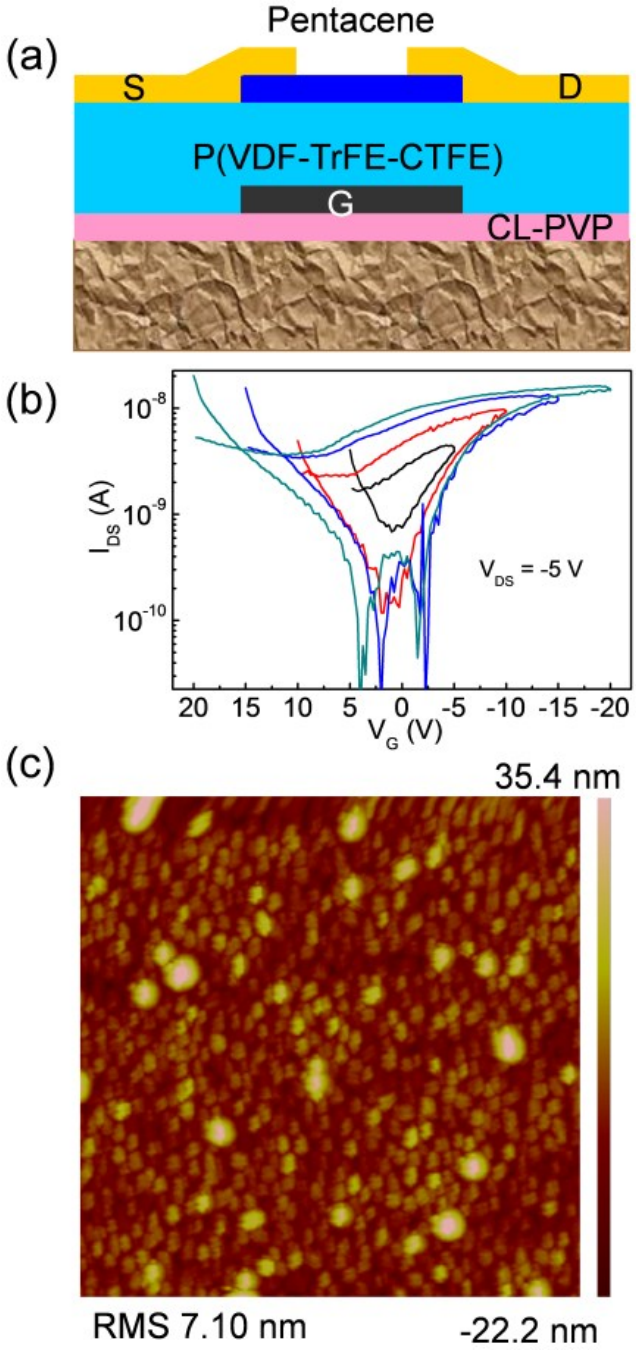

Figure S3. (a) Schematic diagram of the OFET$_{\text{-Ref 1}}$. (b) $I_{DS} - V_G$ transfer characteristics of the OFET$_{\text{-Ref 1}}$ at various V_G sweeping ranges. (c) AFM image of pentacene film deposited on the surface of P(VDF-TrFE-CTFE) film.

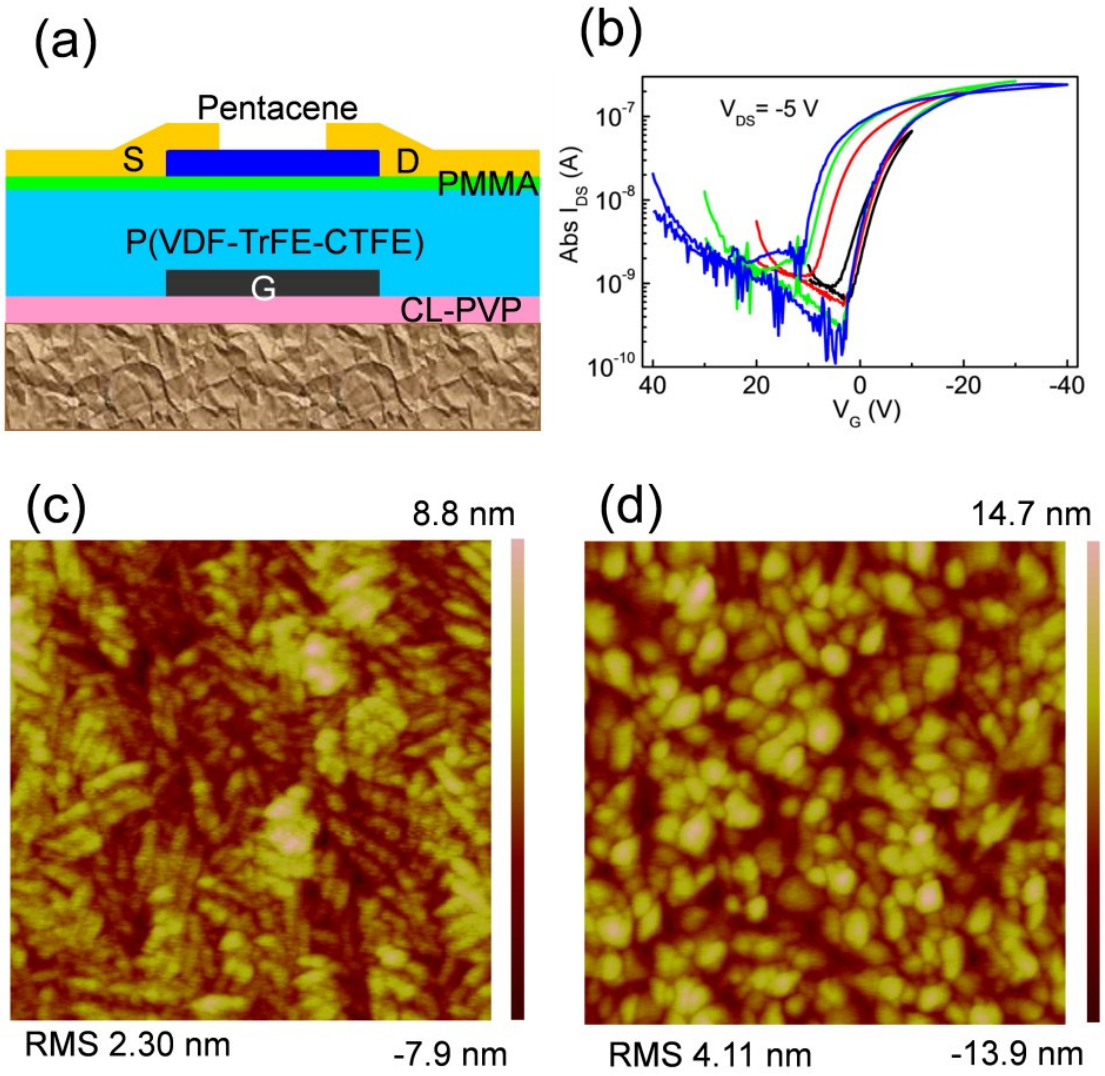

Figure S4. (a) Schematic diagram of the OFET$_{\text{-Ref 2}}$. (b) $I_{DS} - V_G$ transfer characteristics of the OFET$_{\text{-Ref 2}}$ at various V_G sweeping ranges. AFM images of (c) PMMA film spin-coated on the surface of P(VDF-TrFE-CTFE) film and (d) pentacene film deposited on the surface of the discontinuous PMMA film.

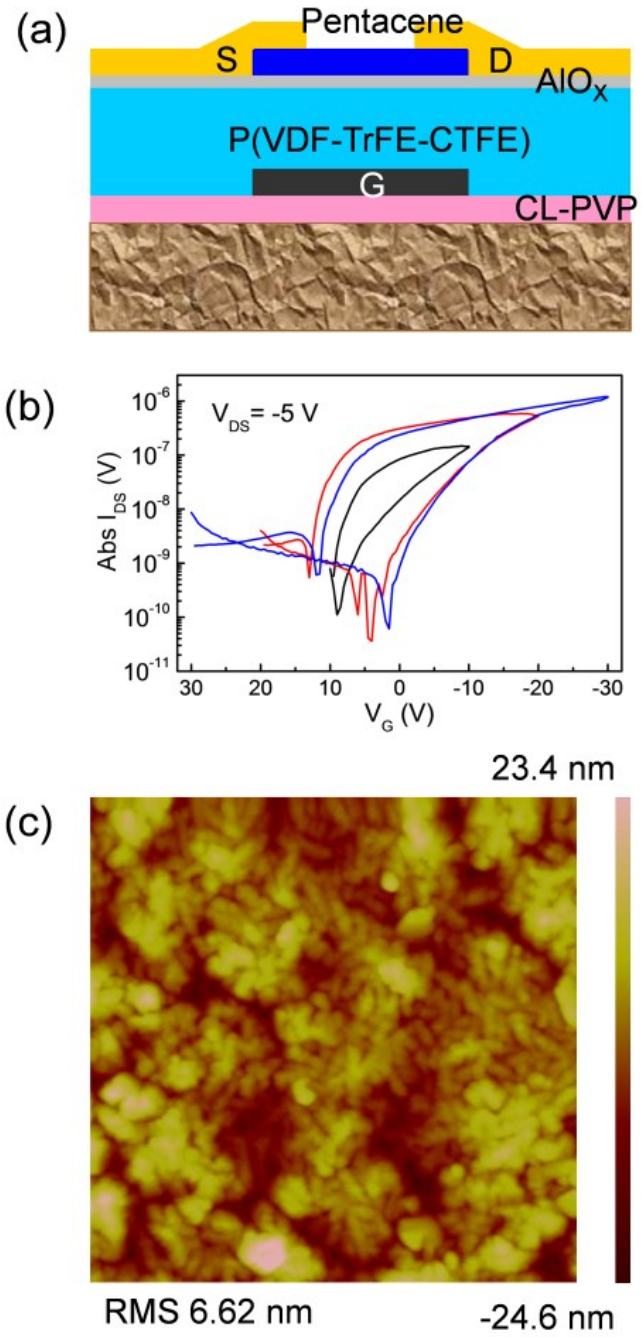

Figure S5. (a) Schematic diagram of the OFET$_{\text{-Ref 3}}$. (b) $I_{DS} - V_G$ transfer characteristics of the OFET$_{\text{-Ref 3}}$ at various V_G sweeping ranges. AFM images of (c) pentacene film deposited on the surface of AlO_X buffer layer.

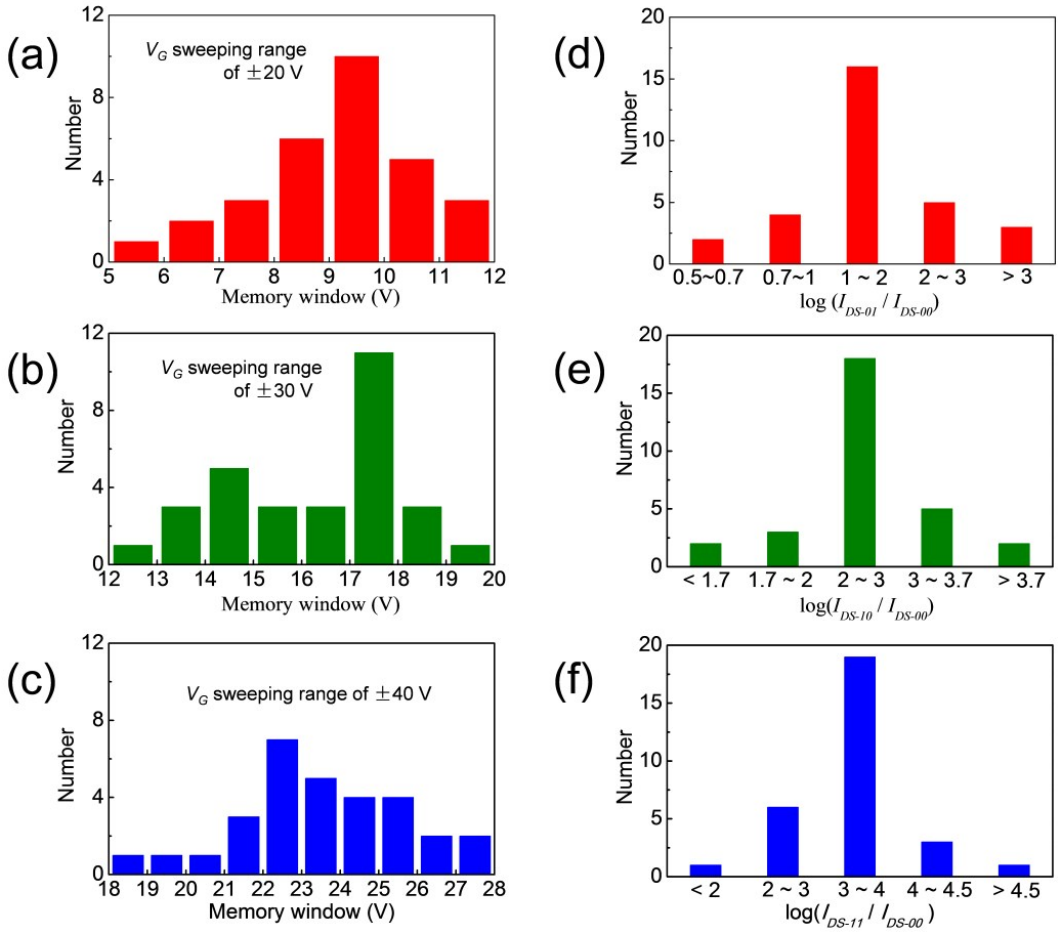

Figure S6. Statistical device population with the memory window extracted at the V_G sweeping ranges of (a) ±20, (b) ±30, and (c) ±40 V, and with the memory on/off ratio on the log scale extracted at the V_G sweeping ranges of (d) ±20, (e) ±30, and (f) ±40 V, obtained from a total of 30 paper-based multi-bit NVMs.

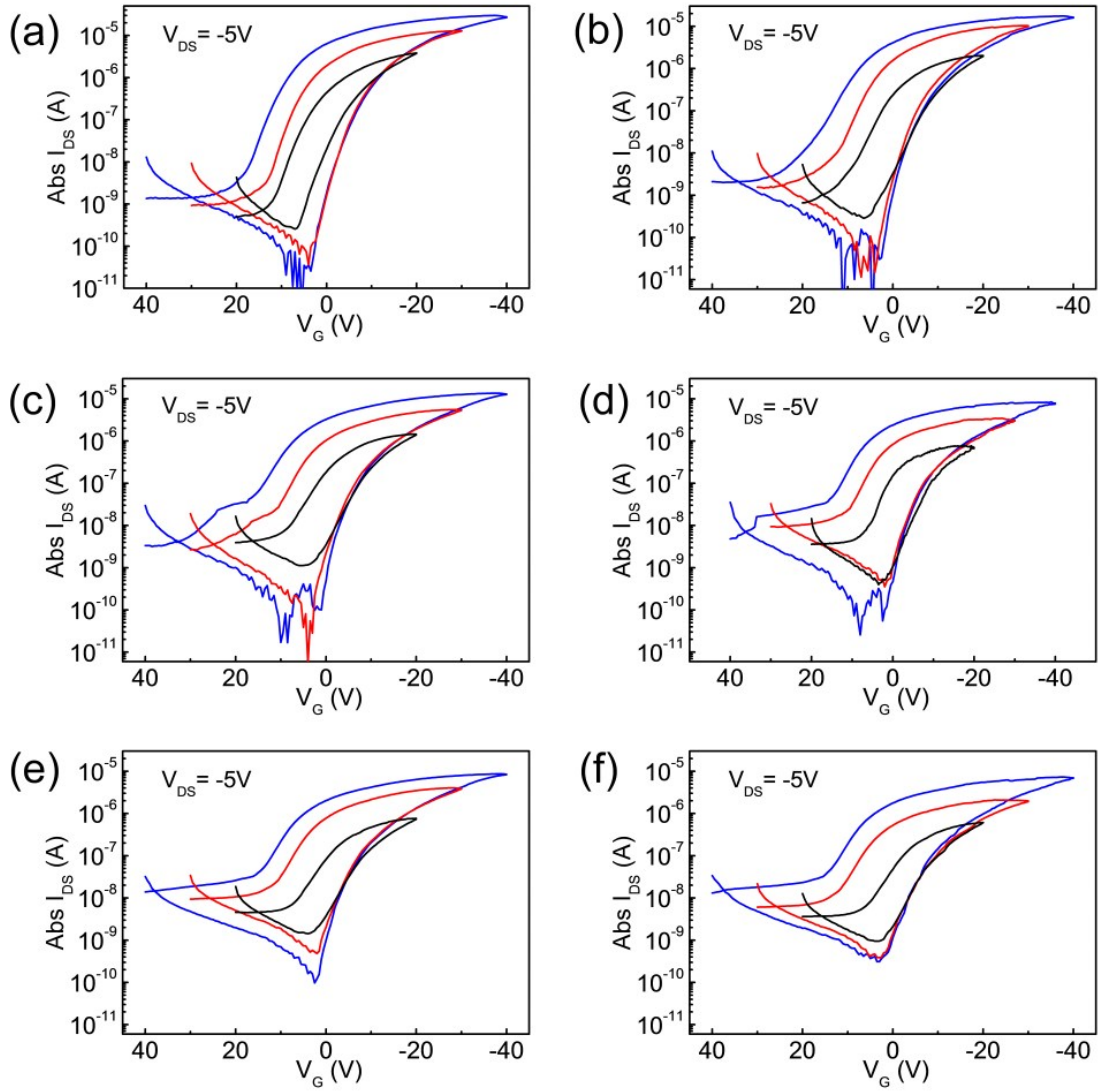

Figure S7. Transfer characteristics of a multi-bit OFET-NVM on paper substrate after implementing (a) 0, (b) 20, (c) 60，(d) 100, (e) 150, and (f) 200 bending cycles at a tensile *r* of 10 mm.

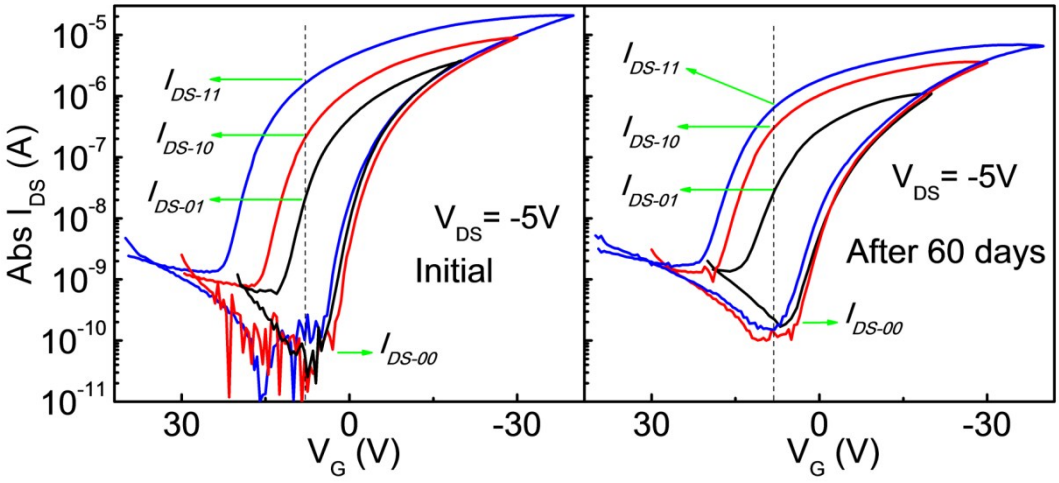

Figure S8. Transfer characteristics of a multi-bit OFET memory measured at its initial period and after 60 days, respectively

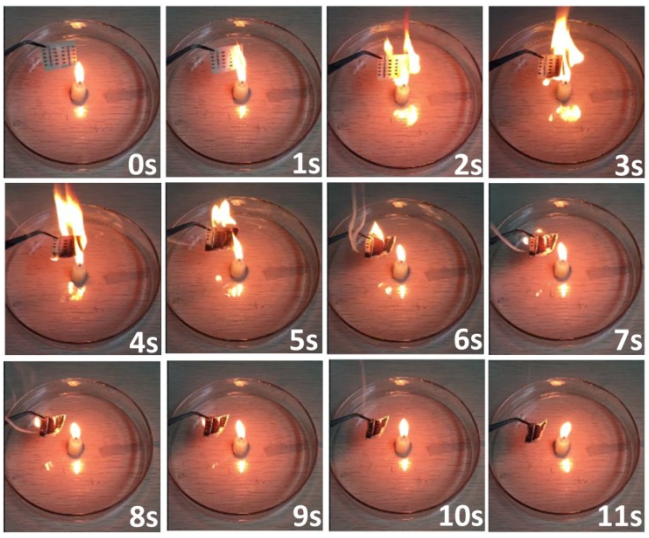

Figure S9. Physical destruction of our 2-bit OFET-NVMs on paper substrate using incineration.

Table S1. Summary of the mobility, ΔV_T and memory on/off ratio of the multi-bit OFET-NVMs operating at different conditions.

Testing conditions		Mobility ($cm^2\ V^{-1}\ s^{-1}$)	$V_G \sim \pm 40$ V		$V_G \sim \pm 30$ V		$V_G \sim \pm 20$ V	
			ΔV_T (V)	Memory on/off ratio*	ΔV_T (V)	Memory on/off ratio*	ΔV_T (V)	Memory on/off ratio*
Bending radius (mm)	50	0.89	27.1	5.4×10^3	17.2	3.4×10^2	9.2	3.2×10^1
	40	0.85	25.1	3.8×10^3	15.8	1.8×10^2	8.5	1.6×10^1
	30	0.73	25.3	3.0×10^3	16.2	3.8×10^2	8.6	1.2×10^1
	20	0.61	24.2	1.8×10^3	16.1	3.6×10^2	8.5	1.2×10^1
	10	0.54	24.1	2.8×10^3	15.8	1.0×10^2	8.4	0.92×10^1
	4	0.22	23.8	9.5×10^3	14.1	1.4×10^2	8.2	1.1×10^1
Humidity	50%	0.91	28.7	2.8×10^4	19.7	6.6×10^3	10.6	1.4×10^2
	58%	0.74	26.9	7.2×10^3	19.3	4.5×10^3	10.4	7.4×10^1
	67%	0.66	26.1	3.1×10^3	18.6	4.7×10^3	9.8	2.5×10^1
	75%	0.42	25.9	6.5×10^2	19.1	2.0×10^3	10.1	3.3×10^1
	83%	0.34	25.3	7.0×10^2	18.4	2.1×10^2	10.7	1.7×10^1
Temperature (ºC)	26	0.36	25.0	1.2×10^3	17.9	1.9×10^2	9.6	1.3×10^1
	50	0.30	20.2	4.6×10^2	15.1	2.0×10^2	7.4	1.5×10^1
	60	0.19	19.7	4.4×10^2	14.8	1.2×10^2	6.5	9.0×10^0
	80	0.18	19.5	2.9×10^2	13.9	2.4×10^1	6.1	3.4×10^0
	100	0.11	19.3	2.2×10^4	13.6	9.1×10^2	5.8	7.5×10^0

* The memory on/off ratio was extracted at the V_G of 5 V.